# Formation and Evolution of Antimatter Objects
# -
# Bled Workshop 2025

July 13, 2025

Sattvik Yadav
*School of Physical Sciences*
*National Institute of Science Education and Research*

# Content

## Search for antimatter stars

- Our universe is overwhelmingly matter-dominated. Research suggest the possibility of exixtence regions of antimatter in our universe. (Chechetkin, Khlopov, and Sapozhnikov, 1982) (Khlopov, Rubin, and Sakharov, 2000) (Blinnikov, Dolgov, and Postnov, 2015)
- Stars are the first objects to form that brought light to the comic dark ages. Thus search for antistars is natural as they will give us the solid confirmation of existence of antimatter in the universe.
- We'll explore stars and antistar in parallel, their formation conditions, theoretical evolution, and detection methods.
- We take the assumption from the start that the thermodynamics is invariant for antimatter.

## What are the properties of the region forming the antistars?

- Local antimatter domain in a matter dominated early universe.
- Period considered at the redshift of $z \approx 20$ or is $0.3$Myr old.
- Total mass of cloud $\approx 10^5 M_\odot$ with antimatter $5\%$, thus $5 \times 10^3 M_\odot$ of antimatter in the cloud
- Temperature of gas cloud $\approx 1000K$.
- Species present for matter regions - $e^-$, $H$, $H^-$, $H^+$, $He$, $He^+$, $He^{++}$, $H_2$, $H_2^+$
  Thus their antimatter counterparts present in the cloud will be $e^+$, $\bar{H}$, $\bar{H}^-$, $\bar{H}^+$, $\bar{H}e$, $\bar{H}e^-$, $\bar{H}e^{--}$, $\bar{H}_2$, $\bar{H}_2^-$
- Mean molecular mass of a gas cloud

$$\mu = \left( \sum_i \frac{X_i(1 + Z_i)}{\mu_i} \right)^{-1}$$

## Density profile of the gas cloud with change in metallicity

Polytropic relation

$$P = K\rho^{1+\frac{1}{n}} \tag{1}$$

The approximate density profile is calculated through the use of Lane-Emden equation

$$\frac{1}{z^2}\frac{d}{dz}\left(z^2\frac{dw}{dz}\right) + w^n = 0 \tag{2}$$

Here,

$$z = Ar$$

$$w^n = \frac{\rho}{\rho_c}$$

$$A^2 = \frac{4\pi G}{(n+1)K}\rho_c^{\frac{n-1}{n}}$$

## Density profile of the gas cloud with change in metallicity

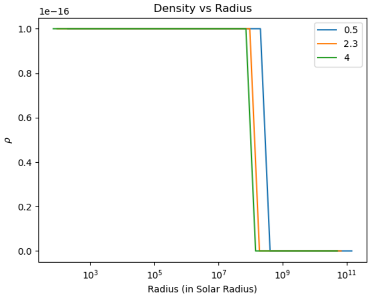


Figure: The figure show the variation of density of a cloud with ideal gas (for ideal gas, $n \to \infty$). The gas in the primordial clouds can be approximately considered as an ideal gas, since a low density gas occupy a large volume. The figure is obtained through plotting the Lane-Emden equation.

## Onset of Collapse

- Initial collapse process occur under isothermal condition. Free fall time - $10^7 yrs$, time taken to reach thermal equilibrium - $10 yrs$. (Kippenhahn and Weigert, 2013)
- The Collapse cloud should satisfy Jeans' conditions

$$M_J = 1.1 M_\odot (\frac{T}{10K})^{\frac{3}{2}} \left(\frac{\rho}{10^{-19} gcm^{-3}}\right)^{-\frac{1}{2}} \left(\frac{\mu}{2.3}\right)^{-\frac{3}{2}}$$

Bonnor-Ebert condition serves as a more realistic condition that takes into account the finiteness of the region of gas under consideration.

$$M_B E = 1.18 \frac{R_H^2}{\mu^2 G^{\frac{3}{2}}} T^2 (P^*)^{-\frac{1}{2}} M_\odot$$

- Both of the above equations will remain symmetric for antimatter based upon the invariance of the thermodynamics as mentioned before.

## Onset of Collapse

Table: Calculated values for the Jeans Mass (JM) and Bonnor Ebert Mass (BEM) for different values of the mean molecular mass $\mu$. We note that the collapse mass required is approximately equal to the JM and BEM of the initial gas cloud of antimatter taken. The $\mu = 0.5$ value is the mean molecular mass calculated for antimatter based upon the chemical abundance of the species mentioned earlier and by considering atomic hydrogen in majority.

| $\mu$ | **Jeans Mass (in $M_\odot$)** | **Bonnor-Ebert Mass (in $M_\odot$)** |
|---|---|---|
| 0.5 | 5581.491579 | 5689.938953 |
| 2.3 | 565.735623 | 1236.943251 |
| 4.0 | 246.669409 | 711.242369 |

## Onset of Collapse

- The atomic hydrogen present aids in the gravitational collapse of the gas cloud. Due to the low opacity value of the gas cloud, the energy radiated is at a high rate.
- Initially the gas cools from $1000K$ to a temperature of $200K$ through $H_2$ formation through $H^-$.

$$H + e^- \rightarrow H^- + h\nu$$

$$H^- + H \rightarrow H_2 + e$$

- This leads to a sharp increase in the fraction of the $H_2$ molecules in the gas cloud as seen in the Figure 2

## Simulating the Collapse

Equations governing the collapse process.(Larson, 1969)
Continuity equation

$$\frac{\partial m}{\partial t} + 4\pi r^2 v \rho = 0 \tag{3}$$

Equation of Motion

$$m\frac{dv}{dt} = F_{grav} + F_{pressure} \tag{4}$$

Angular EQM

$$N = \sum_{i}^{M} r_i (F_{grav} + F_{pressure}) \tag{5}$$

Energy equation

$$\frac{du}{dt} + P\frac{d}{dt}\left(\frac{1}{\rho}\right) + \frac{1}{4\pi\rho r^2}\frac{\partial \Lambda}{\partial r} = 0 \tag{6}$$

## Simulating the Collapse

And finally, the rate of cooling of the gas

$$\left[\Lambda = -\frac{16\pi a c r^2}{3\kappa\rho} T^3 \frac{\partial T}{\partial r}\right]^* \tag{7}$$

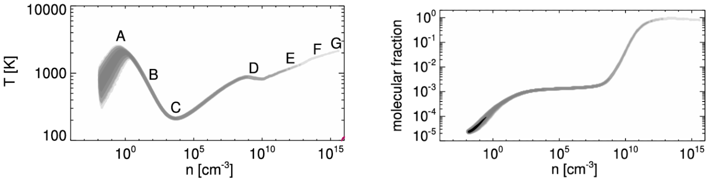


Figure: Variation of the temperature and molecular fraction with the increase in number density as simulated for primordial matter stars (Yoshida et al., 2006).

$$\Lambda_{\rm LTE} = \Lambda_{\rm rot} + \Lambda_{\rm vib},$$

$$\Lambda_{\rm rot} = \frac{9.5 \times 10^{-22} T_3^{3.76}}{1 + 0.12 T_3^{2.1}} \exp\left[-\left(\frac{0.13}{T_3}\right)^3\right] + 3 \times 10^{-24} \exp\left[-\left(\frac{0.51}{T_3}\right)\right]$$

$$\Lambda_{\rm vib} = 6.7 \times 10^{-19} \exp\left[-\left(\frac{5.86}{T_3}\right)\right] + 1.6 \times 10^{-18} \exp\left[-\left(\frac{11.7}{T_3}\right)\right],$$

$$T_3 = \frac{T}{1000\ \rm K}.$$

Figure: Local Thermodynamic Cooling. Cooling process due to de-excitation of atoms from a higher energy state to a lower energy state. (Hollenbach and McKee, 1979)

$$\Lambda_{\rm CIE} = {\rm dex}\Big[-116.6 + 96.34 \log T - 47.153(\log T)^2 + 10.744(\log T)^3 - 0.916(\log T)^4\Big].$$

Figure: Collision induced cooling of hydrogen atoms. (Omukai, 2001)

## Simulating the Collapse

- Later, when the number density species in the gas reach approximately $10^9 cm^{-3}$, where at this stage, 3-body reaction of $H$ start, which almost completely turns the the atomic hydrogen to molecular hydrogen.

$$H + H + H \rightarrow H_2 + H$$

$$H_2 + H \rightarrow 2H_2$$

- Similar reactions must exist for antimatter as well for the such antimatter region to form antistars.
- Due to low density, absence of interstellar dust and lack of opacity of primodial gas, opacity of the surrounding gas is much less than that in the modern universe and thus the rate of cooling is much faster for such environments.

## Process of Protostar Formation

- At the densities of around $10^{12} cm^{-3}$, the gas starts to become opaque, the energy is no longer radiated and is used up in the heating of the gas.
- Due to the increased opacity, density and temperature, the collapse goes from quasi-isothermal to adiabatic, and formation of hydrostatic equilibrium core occurs and thus the formation of protostar.
- The core temperature is enough to ionise the gas and convert it back from molecular to atomic species.

## Simulating the Collapse

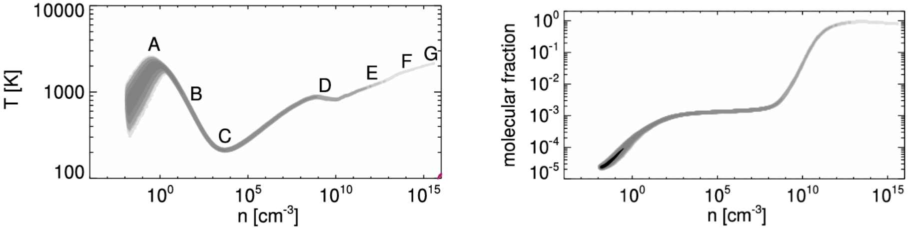


Figure: Variation of the temperature and molecular fraction with the increase in number density as simulated for primordial matter stars, Yoshida et. al. 2006.

## Process of Protostar Formation

- With further increase in temperature, nuclear burning star to occur. For antimatter, the feasibility of such a reaction occurring is a key factor affecting the formation of such stars.

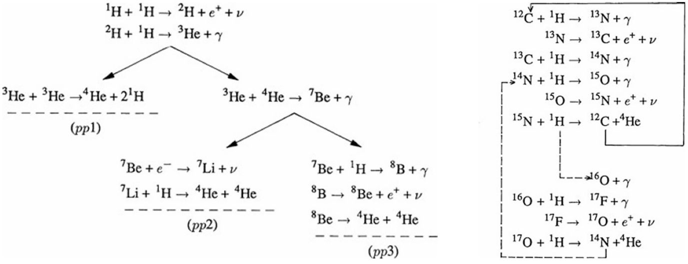


Figure: The following figure shows the major nuclear reactions that start to occur in the core during the nuclear burning. The set of reactions on the left is the ones that start first. The set of reactions on the right is the one that becomes dominant after an increase in metallicity due to fusion reactions.

## Process of Protostar Formation

- The central temperature of the now opaque core varies with the central density according to the following equation

$$\frac{dT_c}{T_c} = \frac{4\alpha - 3}{3\delta}\frac{d\rho_c}{\rho_c} \quad (8)$$

- Matter, if highly compressed, may become degenerate in the region of the core and stop it from having nuclear burning. The boundary region for such is given by

$$\frac{R}{\rho^{\frac{2}{3}}} = \frac{1}{20}\left(\frac{3}{\pi}\right)^{\frac{2}{3}} \frac{h^2}{m_e R_H m_u^{\frac{5}{3}}} \frac{\mu}{\mu_e^{\frac{5}{3}}} \quad (9)$$

- Again analytic analysis reveal that both the condition on the collapsing matter and the degeneracy condition is symmetric for antimatter.

## Process of Protostar Formation

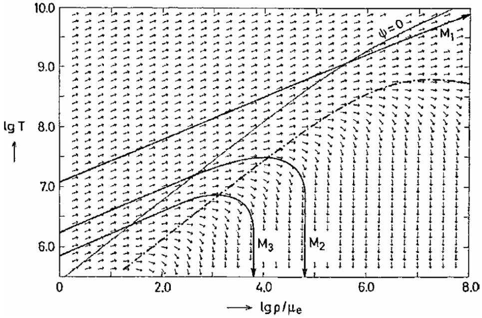


Figure: Graph showing the region determining whether the core becomes degenerate or not.

## Main Sequence

Once the protostar is formed based upon the amount of the rate of mass infall and the feedback created by the nuclear burning, the final mass of the star may be determined.

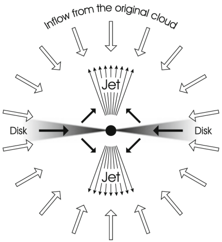


Figure: Depiction of the formed protostar with the accretion disc around the star with the jet of particles from the poles, parts where the accretion is the minimum.

## Main Sequence Star

At the end of the process, we are left with a star. The radiation feedback process blows away or photovapourise the surrounding clouds, and the star is formed. Various papers have put limits on the mass of the star so formed.

- $M_* \approx 100M_\odot$ ($\geq 60M_\odot$) (Yoshida et al., 2006)
- $M_* \approx 42M_\odot$ (Yoshida, Hosokawa, and Omukai, 2012)
- $M_* \geq 22M_\odot$ (Stacy, Greif, and Bromm, 2012)

We note that all the stars formed massive stars, all capable of going supernova of various types, depending upon the mass.

## End of the Star

Stars with different masses end in different ways:

- $140M_{\odot} < M_{*} < 260M_{\odot}$: Pair Instability Supernova: Theoretical supernova predicted to form electron-positron pair, which have a runaway effect of blowing the star appear.
- $40M_{\odot} < M_{*} < 140M_{\odot}$ Supernova forming a black hole.
- $M_{*} < 40M_{\odot}$: Possibility of a neutron star or a black hole

## How to detect antistars?

- Presence of anti-neutron stars or anti-white dwarfs.
- Specific lines in gamma ray spectrum produced due to annihilation of baryon and antibaryon pair. Interaction of specific species, such as $p - \bar{p}$ or $He - \bar{H}e$, etc., will have a specific energy of gamma rays.
- Presence of specific lines in X-Ray spectrum, showing the presence of the atomic systems giving rise to them. These include $p\bar{p}$, $p\bar{H}e$, $He\bar{H}e$, etc. They have a distinct spectrum in the $1 - 10keV$ range.

Promising observations have been made with respect to gamma ray. Dupourqué, Tibaldo, and von Ballmoos, 2021 claims to have found 14 possible signatures of antimatter stars from the observations from Fermi Large Area Telescope.

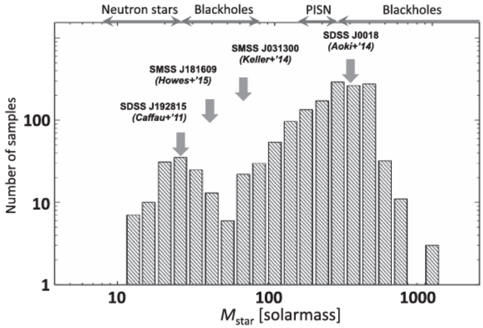


Figure: Figure obtained from the paper shows some of the observed low metallically stars and the simulated distribution of first primordial stars (YOSHIDA, 2019).

## Conclusion

- With the given antimatter abundance, there is possibility of antimatter stars to exist in the early universe.
- The equations derived for the antistar formation from the from the fundamental laws of gravitation and thermodynamics are assumed to be symmetric for antimatter.
- Direct observation of antistar is difficult and requires us to probe in different regions of spectra for such.

# References


1. Kippenhahn, R., & Weigert, A. (2013). Stellar structure and evolution. Springer International Publishing. https://doi.org/10.1007/978-3-642-30304-3
2. Larson, R. B. (1969). Numerical Calculations of the Dynamics of a Collapsing Proto-Star. Monthly Notices of the Royal Astronomical Society, 145(3), 271–295. https://doi.org/10.1093/mnras/145.3.271
3. Stacy, A., Greif, T. H., & Bromm, V. (2012). The first stars: Mass growth under protostellar feedback. Monthly Notices of the Royal Astronomical Society, 422(1), 290–309. https://doi.org/10.1111/j.1365-2966.2012.20605.x
4. Yoshida, N., Hosokawa, T., & Omukai, K. (2012). Formation of the first stars in the universe. Progress of Theoretical and Experimental Physics, 2012(1), 01A305. https://doi.org/10.1093/ptep/pts022
5. Yoshida, N., Omukai, K., Hernquist, L., & Abel, T. (2006). Formation of Primordial Stars in a $\Lambda$CDM Universe. The Astrophysical Journal, 652(1), 6–25. https://doi.org/10.1086/507978
6. Blinnikov, S. I., Dolgov, A. D., & Postnov, K. A. (2015). Antimatter and antistars in the Universe and in the Galaxy. Phys. Rev. D, 92(2), 023516. https://doi.org/10.1103/PhysRevD.92.023516
7. Khlopov, M. Y., Rubin, S. G., & Sakharov, A. S. (2000). Possible origin of antimatter regions in the baryon dominated universe. Phys. Rev. D, 62(8), 083505. https://doi.org/10.1103/PhysRevD.62.083505
8. Hollenbach, D.,& McKee, C. F. (1979). Molecule formation and infrared emission in fast interstellar shocks. I. Physical processes. The Astrophysical Journal Supplement Series, 41(3), 555–592. https://doi.org/10.1086/190631
9. Omukai, K. (2001). Primordial Star Formation under Far-Ultraviolet Radiation. The Astrophysical Journal, 546(2), 635–651. https://doi.org/10.1086/318296
10. Dupourqué, S., Tibaldo, L., & von Ballmoos, P. (2021). Constraints on the antistar fraction in the Solar System neighborhood from the 10-year Fermi Large Area Telescope gamma-ray source catalog. Physical Review D, 103(8), 083016. https://doi.org/10.1103/PhysRevD.103.083016
11. ReferencesChechetkin, V. M., Khlopov, M. Yu., & Sapozhnikov, M. G. (1982). Antiproton interactions with light elements as a test of GUT cosmology. La Rivista Del Nuovo Cimento, 5(10), 1–79. https://doi.org/10.1007/bf02740484

# Thank you!